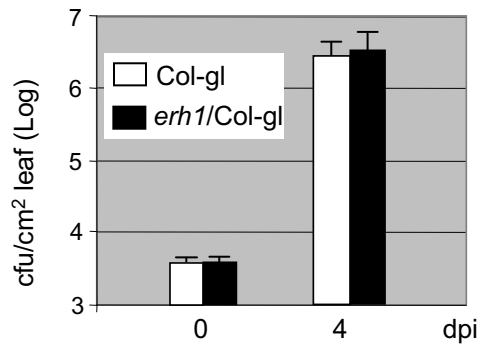
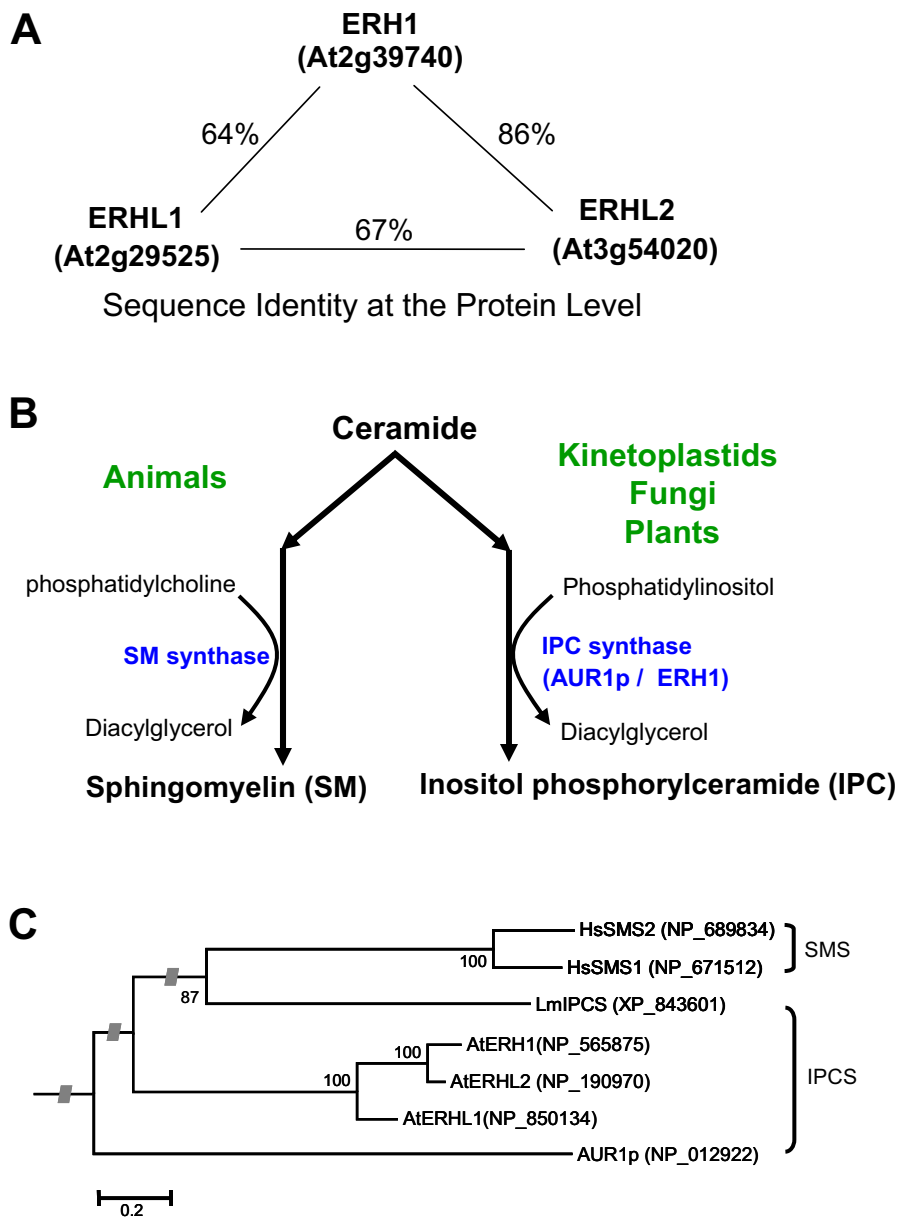


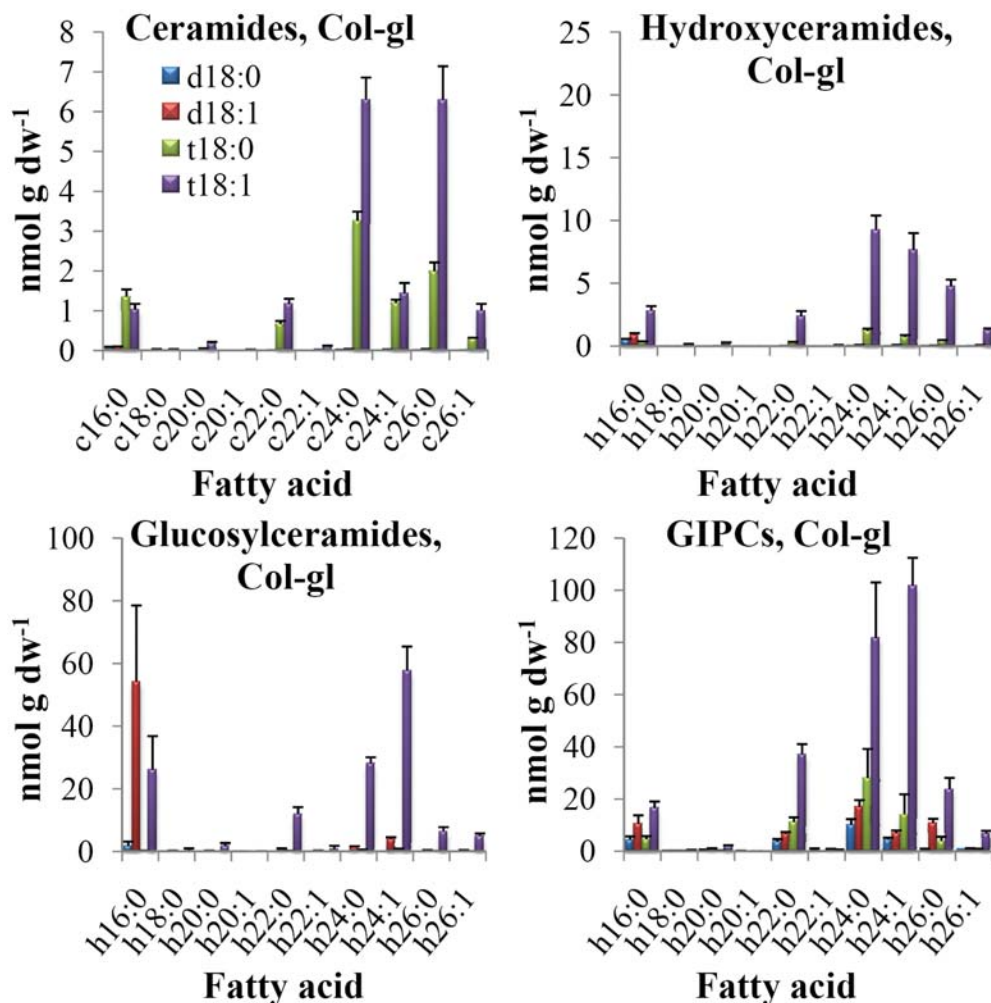
Supplemental Data. Wang et al. (2008) An Inositolphosphorylceramide Synthase Is Involved in Regulation of Plant Programmed Cell Death Associated with Defense in Arabidopsis



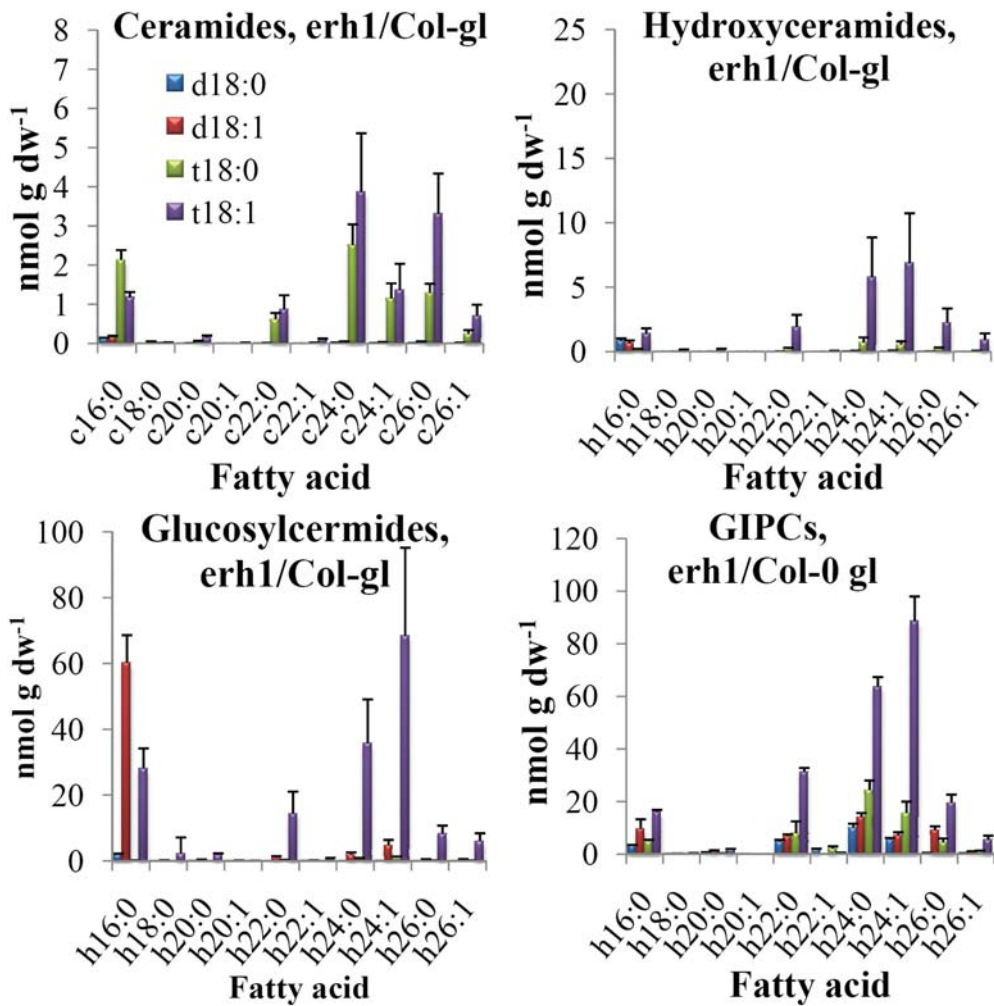
Supplemental Figure 1. *erh1*/Col-gl Plants Are Not More Resistant to *P. syringae*. Five week-old plants were infiltrated with $OD_{600}=0.0002$ *Psm* ES4326. Growth of the bacteria was assayed at 0 and 4 days post-inoculation (dpi). This experiment was repeated two times with similar results. Data are means \pm SE from one experiment. No significant difference ($p>0.50$, $n=3$) is detected between the two genotypes CfU, colony-forming units.



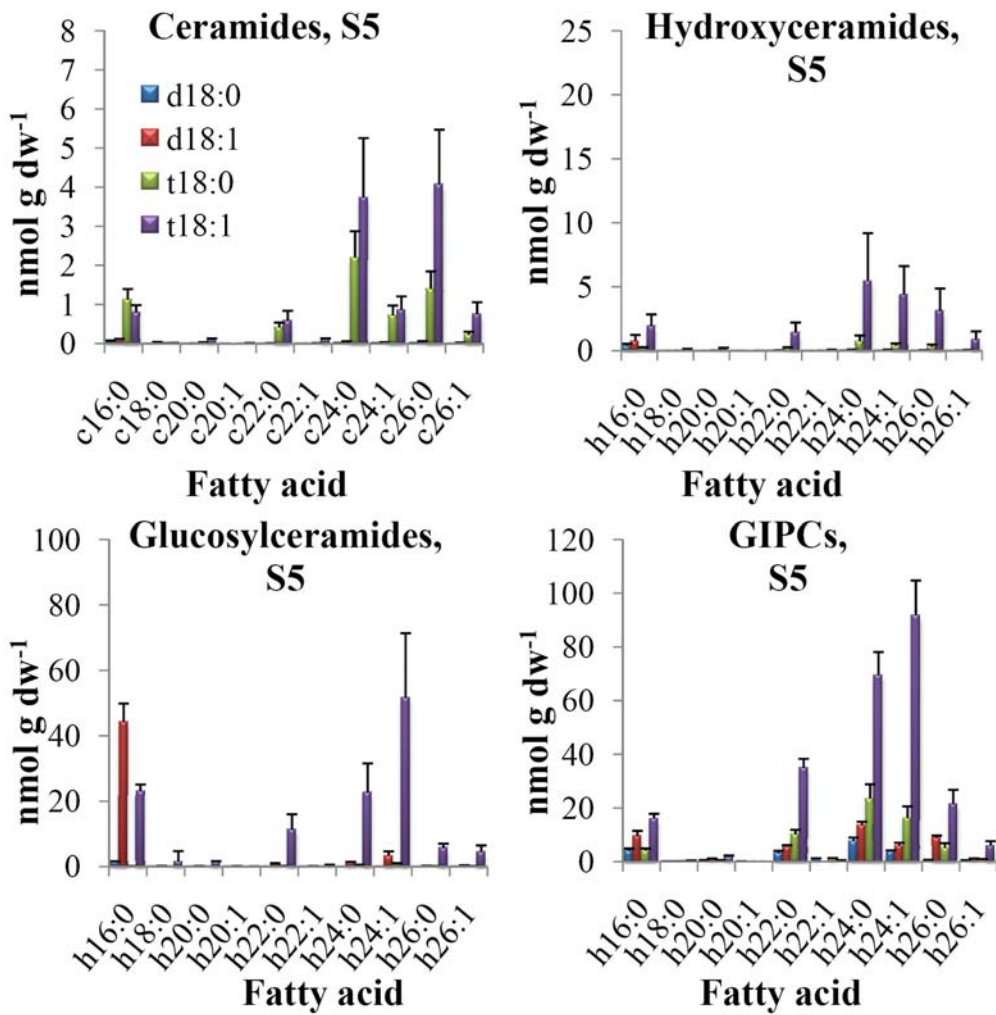
Supplemental Figure 2. Evolution and Diversification of IPCSs (SMSs). **(A)** Sequence similarity between ERH1 and its two homologs in Arabidopsis. **(B)** A dichotomic diversification at the initial step of ceramide metabolism between plants/fungi/kinetoplastid protozoa and animals. Adapted from Denny and Smith (2004). **(C)** A neighbor-joining tree of the SMS and IPCS proteins from different organisms constructed using MEGA4.1 using Poisson correction. Bootstrap proportions of 500 bootstrap replicates >70 are indicated under the branches. Grey bar indicates a likely evolutionary split. Note sequence alignment was done using ClustalW and only the sequences aligned to amino acids 1 to 276 of ERH1 were used for phylogenetic analysis because sequences beyond are very divergent.



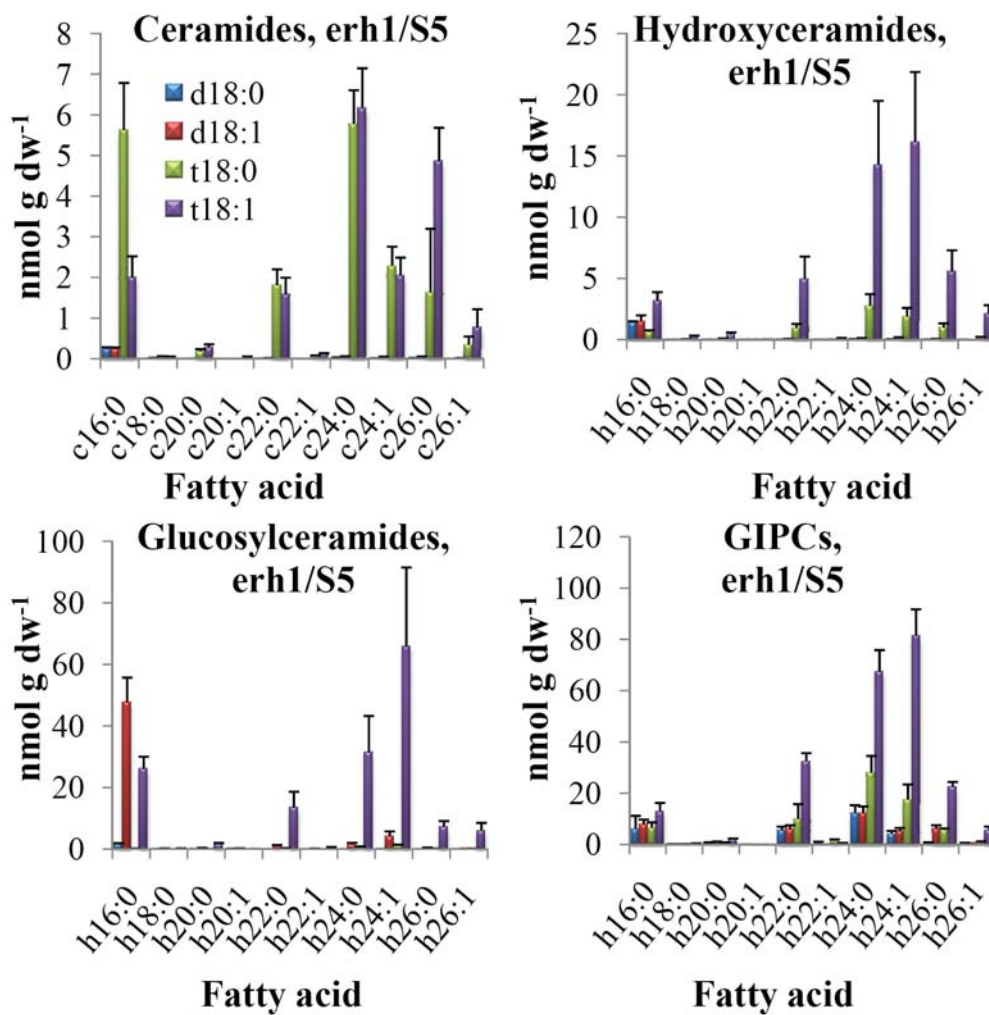
Supplemental Figure 3A. Levels of The Indicated Sphingolipid Species in Leaves of Col-gl Plants. Sphingolipid extracts were determined by HPLC-ESI-MS/MS. Molecular species of individual sphingolipid are indicated long-chain base (LCB) – fatty acid pairings. LCBs consist of sphinganine (d18:0), Δ 8-sphingosine (d18:1), phytosphingosine (t18:0) and Δ 8-phytosphingenine. Fatty acid structures are indicated by carbon atoms (c16-c26), followed by the number of double bonds (0 or 1), the presence of a 2-hydroxy group is indicated by a 'h'.



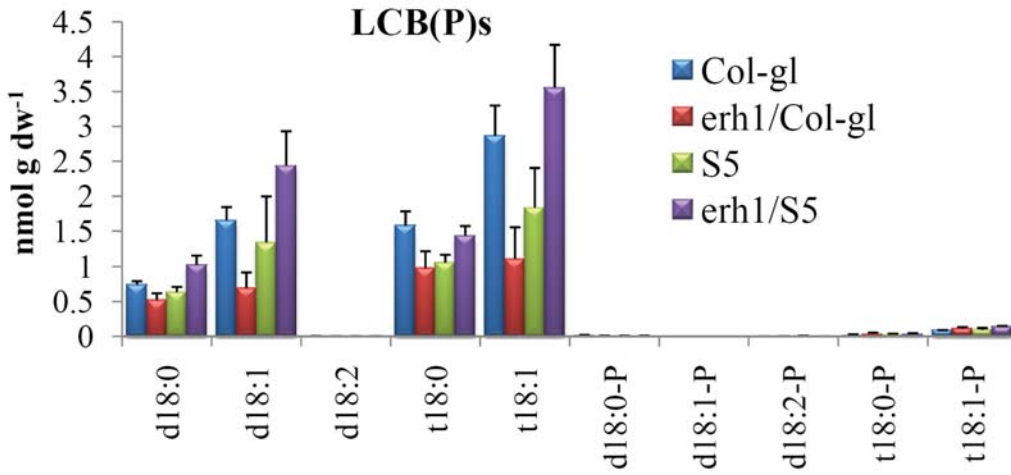
Supplemental Figure 3B. Levels of The Indicated Sphingolipid Species in Leaves of *erh1/Col-gl* Plants. Sphingolipid extracts were determined by HPLC-ESI-MS/MS.



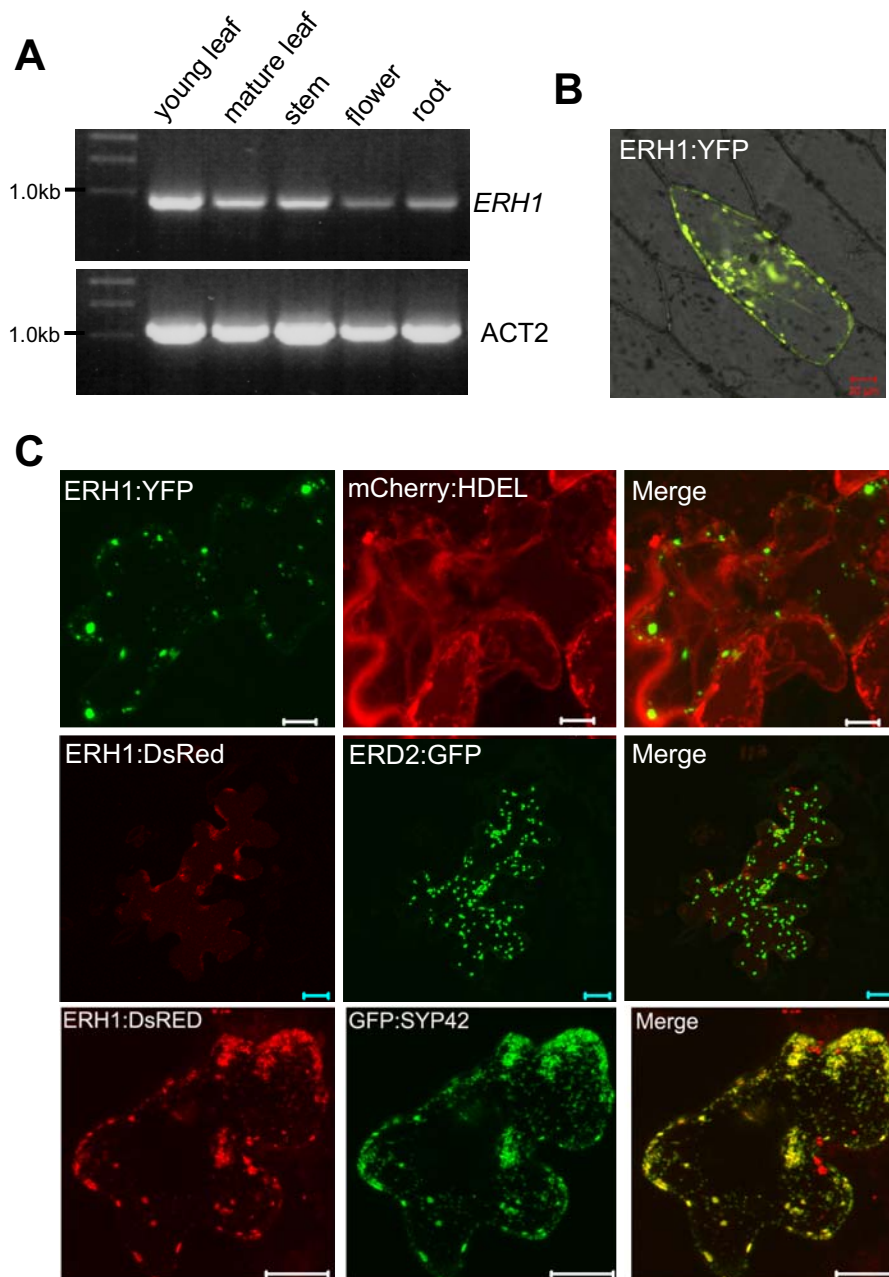
Supplemental Figure 3C. Levels of The Indicated Sphingolipid Species in Leaves of S5 Plants. Sphingolipid extracts were determined by HPLC-ESI-MS/MS.



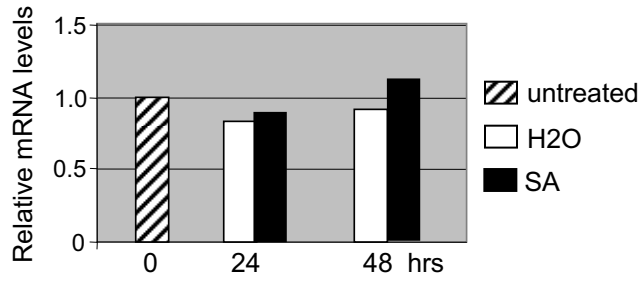
Supplemental Figure 3D. Levels of The Indicated Sphingolipid Species in Leaves of *erh1/S5* Plants. Sphingolipid extracts were determined by HPLC-ESI-MS/MS.



Supplemental Figure 3E. Levels of Sphingoid Long Chain Bases and Their Phosphorylated Derivatives LCB(P)s in the leaves of the indicated plants. Sphingolipid extracts were determined by HPLC-ESI-MS/MS.



Supplemental Figure 4. Expression and Subcellular Localization of ERH1. **(A)** mRNA expression pattern of *ERH1*. RT-PCR was performed using mRNA extracted from different organs of Col-gl. **(B)** Biolistic transient expression of ERH1:YFP in onion epidermal cells. Note the punctate distribution of fluorescence. **(C)** Biolistic co-transient expression of ERH1:DsRed or ERH1:YFP with indicated the ER marker (mCherry:AtWAK2:HEDL), the Golgi marker (ERD2:GFP), and the TGN marker (GFP:SYP42) in Arabidopsis (Col-0) leaves. All the constructs in **(B)** and **(C)** were under control of the 35S promoter and all the pictures were taken 24 hrs after bombardment using a laser scanning confocal microscopy. Scale bar = 10 μ m.



Supplemental Figure 5. *ERH1* Is Not Significantly Induced by SA. cDNA was synthesized from RNA extracted from leaf tissues of Col-0 plants sprayed with water or 0.5 mM SA for transcript quantification by real-time RT-PCR. The relative mRNA levels were calculated relative to that of Col-0 before treatment. This experiment was repeated once with similar data.